Journal of Computational Mathematics, Vol.20, No.1, 2002, 1–14.

A HIGHLY ACCURATE NUMERICAL METHOD FOR FLOW PROBLEMS WITH INTERACTIONS OF DISCONTINUITIES*[1)]

Xiao-nan Wu
(*Department of Mathematics, Hong Kong Baptist University, Kowloon Tong, Hong Kong*)

You-lan Zhu
(*Department of Mathematics, University of North Carolina at Charlotte, Charlotte, NC 28223*)

Abstract

A type of shock fitting method is used to solve some two and three dimensional flow problems with interactions of various discontinuities. The numerical results show that high accuracy is achieved for the flow field, especially at the discontinuities. Comparisons with the Lax-Friedrichs scheme and the ENO scheme confirm the accuracy of the method.

Key words: Interaction of discontinuity, Shock-fitting, Shock-capturing.

1. Introduction

Compared with the widely used shock capturing methods for the compressible flows, the shock fitting methods have the main advantage of accuracy. The shock fitting methods are usually very accurate wherever it can be applied. Several kinds of shock fitting methods have been developed in the last three decades. Glimm and his coworkers have worked extensively on the front tracking methods and applied them to many complicated problems with shocks and other types of singularities [1]-[6]. Moretti [7] has also obtained some very accurate results for gas dynamics problems using his shock fitting method. Mao [8] also developed a front tracking technique for two dimensional problems. In [9]-[10] we developed a technique called the singularity separating method by which the interactions of discontinuities in three dimensional steady supersonic flow has been accurately computed. In [13] we extended the singularity separating method to unsteady two and three dimensional shock reflection problems and obtained very accurate numerical results. The main idea of the singularity separating method is that the computational domain is transformed into sub-domains in which the discontinuities are fixed boundaries. In return, the transformations are time dependent. The flow fields on the two sides of the discontinuities are related by the shock jump conditions or other relations the discontinuities should satisfy. The equations are discretized in each of the sub-domains and no differentiations are performed across the discontinuities. In this way, the high accuracy is achieved both away and at the discontinuities.

In this paper, we extend the method developed in [13] to more complicated problems with interactions of various discontinuities. In section 2, we show the treatment of the interactions of discontinuities. In section 3, we give the algorithms. In section 4, we show two examples of two

* Received May 19, 1998; Final revised July 12, 2000.

[1)] The work was supported in part by the North Carolina Supercomputing Center, the RGC of Hong Kong, and the FRG of Hong Kong Baptist University.

and three dimensional problems with interactions of discontinuities and compare the numerical results with the results obtained from Lax-Friedrichs and ENO schemes.

2. Interactions of Discontinuities

We consider an inviscid flow with some discontinuities in a three dimensional rectangular channel. For simplicity, we assume that at the beginning there are only two discontinuities in the channel. As the time increases, the two discontinuities will get closer, and interact. The governing equation is the three dimensional Euler equation:

$$\frac{\partial \tilde{U}}{\partial t} + \tilde{P}\frac{\partial \tilde{U}}{\partial x} + \tilde{Q}\frac{\partial \tilde{U}}{\partial y} + \tilde{R}\frac{\partial \tilde{U}}{\partial z} = 0, \tag{1}$$

where $\tilde{U} = (p, u, v, w, \rho)^T$,

$$\tilde{P} = \begin{pmatrix} u & \rho a^2 & 0 & 0 & 0 \\ 1/\rho & u & 0 & 0 & 0 \\ 0 & 0 & u & 0 & 0 \\ 0 & 0 & 0 & u & 0 \\ 0 & \rho & 0 & 0 & u \end{pmatrix}, \tilde{Q} = \begin{pmatrix} v & 0 & \rho a^2 & 0 & 0 \\ 0 & v & 0 & 0 & 0 \\ 1/\rho & 0 & v & 0 & 0 \\ 0 & 0 & 0 & v & 0 \\ 0 & 0 & \rho & 0 & v \end{pmatrix}, \tilde{R} = \begin{pmatrix} w & 0 & 0 & \rho a^2 & 0 \\ 0 & w & 0 & 0 & 0 \\ 0 & 0 & w & 0 & 0 \\ 1/\rho & 0 & 0 & w & 0 \\ 0 & 0 & 0 & \rho & w \end{pmatrix},$$

a^2 denoting $\gamma p/\rho$ (in our computation $\gamma = 1.4$).

The initial conditions at $t = 0$ are given by

$$\begin{aligned} &p(x,y,z,0) = p_n(x,y,z), \quad u(x,y,z,0) = u_n(x,y,z), \quad v(x,y,z,0) = v_n(x,y,z), \\ &w(x,y,z,0) = w_n(x,y,z), \quad \rho(x,y,z,0) = \rho_n(x,y,z), \\ &\text{for } \tilde{g}_{n-1}(y,z) \le x \le \tilde{g}_n(y,z),\ -y_b \le y \le y_b,\ -z_b \le z \le z_b,\ n = 1,2,3, \end{aligned}$$

where $p_n(x,y,z)$, $u_n(x,y,z)$, $v_n(x,y,z)$, $w_n(x,y,z)$ and $\rho_n(x,y,z)$, $n = 1,2,3$, are given functions, $\tilde{g}_0(y,z) = 0$ is the left boundary, $\tilde{g}_1(y,z)$ and $\tilde{g}_2(y,z)$ are the two discontinuities, and $\tilde{g}_3(y,z) = 1$ is the right boundary. The flow fields on the two sides of a shock must satisfy the jump conditions:

$$\rho_0(V_{0n} - s) = \rho_1(V_{1n} - s), \tag{2}$$

$$p_0 + \rho_0(V_{0n} - s)^2 = p_1 + \rho_1(V_{1n} - s)^2, \tag{3}$$

$$V_{0t1} = V_{1t1}, \qquad V_{0t2} = V_{1t2}, \tag{4}$$

$$\frac{1}{2}(V_{0n} - s)^2 + \frac{\gamma p_0}{(\gamma - 1)\rho_0} = \frac{1}{2}(V_{1n} - s)^2 + \frac{\gamma p_1}{(\gamma - 1)\rho_1}, \tag{5}$$

where s is the shock speed, V_{0n} and V_{1n} denote the velocities normal to the shock on the two sides of the shock, and V_{0t1}, V_{0t2}, V_{1t1}, and V_{1t2} denote the two linearly independent components

of the velocity tangent to the shock on the two sides of the shock. The flow fields on the two sides of a contact discontinuity must satisfy the jump conditions

$$p_0 = p_1, \qquad V_{0n} = s, \qquad V_{1n} = s, \tag{6}$$

where s is the speed of the contact discontinuity. The boundary conditions are given as follows: on the walls, the velocities normal to the boundaries are set to zero: $V_n(x, y, z, t) = 0$. On the left and right ends of the channel, suitable boundary conditions are also given.

The two discontinuities separate the domain into three sub-domains. Therefore, we introduce a transformation to transform the three sub-domains into three fixed sub-domains, with the two discontinuities as the fixed boundaries of the new sub-domains. In return, the transformation is time dependent. Bearing in mind that we will deal with more complicated situations after the interactions of the discontinuities, in which more discontinuities may appear, we introduce the following transformation

$$\xi = \frac{x - g_{n-1}(\eta, \zeta, \tau)}{g_n(\eta, \zeta, \tau) - g_{n-1}(\eta, \zeta, \tau)} + n - 1, \qquad g_{n-1} \le x \le g_n, \quad n = 1, 2, \cdots, N,$$
$$\eta = \frac{y + y_b}{2y_b}, \qquad \zeta = \frac{z + z_b}{2z_b}, \qquad \tau = \tau_i + (t - k_i(\eta, \zeta))\frac{h_i(0,0) - \tau_i}{h_i(\eta, \zeta) - k_i(\eta, \zeta)},$$

where τ_i is a constant, N is the number of sub-domains separated by the discontinuities, $g_0(\eta, \zeta, \tau) = 0$ is the left boundary, $g_k(\eta, \zeta, \tau)$, $k = 1, 2, \cdots, N-1$, are the x coordinates of the discontinuities for given η, ζ, and τ, $g_N(\eta, \zeta, \tau) = 1$ is the right boundary of the channel, and $h_i(\eta, \zeta)$, $k_i(\eta, \zeta)$ are functions which will be chosen during the computation so that the two discontinuities interact at the same τ for all y and z, or equivalently for all η and ζ. It is easy to see the following: the plane $\xi = 0$ is the left boundary, the planes $\xi = 1, 2, \cdots, N-1$ are the discontinuities, and the plane $\xi = N$ is the right boundary in the (ξ, η, ζ, τ) coordinate system; the planes $\eta = 0$, $\eta = 1$, $\zeta = 0$ and $\zeta = 1$ are the wall boundaries.

Under this transformation, the equations (1) become

$$W\frac{\partial U}{\partial \tau} + P\frac{\partial U}{\partial \xi} + Q\frac{\partial U}{\partial \eta} + R\frac{\partial U}{\partial \zeta} = 0, \tag{7}$$

where

$$U(\xi, \eta, \zeta, \tau) = \tilde{U}(x(\xi, \eta, \zeta, \tau), y(\xi, \eta, \zeta, \tau), z(\xi, \eta, \zeta, \tau), t(\xi, \eta, \zeta, \tau)),$$
$$W = \tau_t I + \tau_x \tilde{P} + \tau_y \tilde{Q} + \tau_z \tilde{R}, \qquad P = \xi_t I + \xi_x \tilde{P} + \xi_y \tilde{Q} + \xi_z \tilde{R},$$
$$Q = \eta_t I + \eta_x \tilde{P} + \eta_y \tilde{Q} + \eta_z \tilde{R}, \qquad R = \zeta_t I + \zeta_x \tilde{P} + \zeta_y \tilde{Q} + \zeta_z \tilde{R}.$$

3. The Discretization of the Transformed Equations

Let $(\cos\theta_1, \cos\theta_2, \cos\theta_3, -\lambda)$ denote the normal direction of a characteristic surface satisfying the equation

$$|P\cos\theta_1 + Q\cos\theta_2 + R\cos\theta_3 - \lambda W| = 0.$$

Let $G_l^T, l = 1, \cdots, 5$, denote the characteristic combination coefficients corresponding to $\lambda_l, l = 1, \cdots, 5$, which satisfy the equations

$$G_l^T (P \cos\theta_1 + Q \cos\theta_2 + R \cos\theta_3 - \lambda_l W) = 0, \quad l = 1, \cdots, 5. \tag{8}$$

Then the five characteristic-compatibility relations can be obtained through multiplying equations (7) by G_l^T, $l = 1, \cdots, 5$,

$$G_l^T \left(W \frac{\partial U}{\partial \tau} + P \frac{\partial U}{\partial \xi} + Q \frac{\partial U}{\partial \eta} + R \frac{\partial U}{\partial \zeta} \right) = 0, \quad l = 1, \cdots, 5. \tag{9}$$

The discretization is performed for equation (9). On the (ξ, η, ζ) plane the mesh is uniform and the mesh sizes are $\Delta\xi$, $\Delta\eta$ and $\Delta\zeta$. The step size $\Delta\tau$ in the τ direction is dependent on the time. Let $U_{i,j,k}^m$ denote the approximate value of U at the grid point $(\xi_i, \eta_j, \zeta_k, \tau_m)$ with $\xi_i = i\Delta\xi$, $\eta_j = j\Delta\eta$, $\zeta_k = k\Delta\zeta$ and $\tau_m = \Delta\tau_0 + \Delta\tau_1 + \cdots + \Delta\tau_{m-1}$. The value of U at $(\xi_i, \eta_j, \zeta_k, \tau_{m+1/2} = \tau_m + \Delta\tau_m/2)$ is denoted by $U_{i,j,k}^{m+1/2}$.

An explicit scheme and a mixed implicit-explicit scheme are used in the computation. The explicit scheme is described as follows: Let $\cos\theta_1 = 1$, $\cos\theta_2 = 0$, $\cos\theta_3 = 0$ and consider the case $\lambda_l > 0$. We change equations (9) to the following form

$$G_l^T \left(W \left(\frac{\partial U}{\partial \tau} + \frac{\Delta\xi}{\Delta\tau_m} \frac{\partial U}{\partial \xi} \right) + \left(P - \frac{\Delta\xi}{\Delta\tau_m} W \right) \frac{\partial U}{\partial \xi} + Q \frac{\partial U}{\partial \eta} + R \frac{\partial U}{\partial \zeta} \right) = 0, \ 1 \le l \le 5. \tag{10}$$

Based on this equation, we have the following scheme,

interim step:

$$\begin{aligned} G_l^T W U_{i,j+1/2,k+1/2}^{m+1/2} = G_l^T \Bigg(& \frac{W}{8} (U_{i,j,k}^m + U_{i-1,j,k}^m + U_{i,j+1,k}^m + U_{i-1,j+1,k}^m + U_{i,j,k+1}^m \\ & + U_{i-1,j,k+1}^m + U_{i,j+1,k+1}^m + U_{i-1,j+1,k+1}^m) - \frac{\Delta\tau_m}{2} \left(P - \frac{\Delta\xi}{\Delta\tau_m} W \right) \cdot \\ & \Delta_\xi U_{i-1/2,j+1/2,k+1/2}^m - \frac{\Delta\tau_m}{2} \left(Q \Delta_\eta U_{i-1/2,j+1/2,k+1/2}^m + R \Delta_\zeta U_{i-1/2,j+1/2,k+1/2}^m \right) \Bigg) \end{aligned}$$

with

$$\begin{aligned} \Delta_\xi U_{i-1/2,j+1/2,k+1/2}^m = & \frac{1}{4\Delta\xi} \left((U_{i,j,k}^m + U_{i,j+1,k}^m + U_{i,j,k+1}^m + U_{i,j+1,k+1}^m) \right. \\ & \left. - (U_{i-1,j,k}^m + U_{i-1,j+1,k}^m + U_{i-1,j,k+1}^m + U_{i-1,j+1,k+1}^m) \right) \\ \Delta_\eta U_{i-1/2,j+1/2,k+1/2}^m = & \frac{1}{4\Delta\eta} \left((U_{i,j+1,k}^m + U_{i-1,j+1,k}^m + U_{i,j+1,k+1}^m + U_{i-1,j+1,k+1}^m) \right. \\ & \left. - (U_{i,j,k}^m + U_{i-1,j,k}^m + U_{i,j,k+1}^m + U_{i-1,j,k+1}^m) \right) \\ \Delta_\zeta U_{i-1/2,j+1/2,k+1/2}^m = & \frac{1}{4\Delta\zeta} \left((U_{i,j,k+1}^m + U_{i-1,j,k+1}^m + U_{i,j+1,k+1}^m + U_{i-1,j+1,k+1}^m) \right. \\ & \left. - (U_{i,j,k}^m + U_{i-1,j,k}^m + U_{i,j+1,k}^m + U_{i-1,j+1,k}^m) \right); \end{aligned}$$

regular step:

$$G_l^T W U_{i,j,k}^{m+1} =$$
$$G_l^T \left(W U_{i-1,j,k}^m - \Delta\tau_m \left(\left(P - \frac{\Delta\xi}{\Delta\tau_m} W \right) \Delta_\xi U_{i-1/2,j,k}^{m+1/2} + Q \Delta_\eta U_{i-1/2,j,k}^{m+1/2} + R \Delta_\zeta U_{i-1/2,j,k}^{m+1/2} \right) \right),$$

where G_l^T and all the matrices are evaluated at $(\xi_{i-1/2}, \eta_{j+1/2}, \zeta_{k+1/2}, \tau_m)$ for the interim step and at $(\xi_{i-1/2}, \eta_j, \zeta_k, \tau_{m+1/2})$ for the regular step.

For $\lambda_l < 0$ we change equations (9) to the following form

$$G_l^T \left(W \left(\frac{\partial U}{\partial \tau} - \frac{\Delta\xi}{\Delta\tau_m} \frac{\partial U}{\partial \xi} \right) + \left(P + \frac{\Delta\xi}{\Delta\tau_m} W \right) \frac{\partial U}{\partial \xi} + Q \frac{\partial U}{\partial \eta} + R \frac{\partial U}{\partial \zeta} \right) = 0,\ 1 \le l \le 5. \qquad (11)$$

This equation can be discretized in the following way,

interim step:

$$G_l^T W U_{i,j+1/2,k+1/2}^{m+1/2} = G_l^T \left(\frac{W}{8} (U_{i+1,j,k}^m + U_{i,j,k}^m + U_{i+1,j+1,k}^m + U_{i,j+1,k}^m + U_{i+1,j,k+1}^m \right.$$
$$+ U_{i,j,k+1}^m + U_{i+1,j+1,k+1}^m + U_{i,j+1,k+1}^m) - \frac{\Delta\tau_m}{2} \left(P + \frac{\Delta\xi}{\Delta\tau_m} W \right) \cdot$$
$$\left. \Delta_\xi U_{i+1/2,j+1/2,k+1/2}^m - \frac{\Delta\tau_m}{2} \left(Q \Delta_\eta U_{i+1/2,j+1/2,k+1/2}^m + R \Delta_\zeta U_{i+1/2,j+1/2,k+1/2}^m \right) \right);$$

regular step:

$$G_l^T W U_{i,j,k}^{m+1} =$$
$$G_l^T \left(W U_{i+1,j,k}^m - \Delta\tau_m \left(\left(P + \frac{\Delta\xi}{\Delta\tau_m} W \right) \Delta_\xi U_{i+1/2,j,k}^{m+1/2} + Q \Delta_\eta U_{i+1/2,j,k}^{m+1/2} + R \Delta_\zeta U_{i+1/2,j,k}^{m+1/2} \right) \right),$$

where G_l^T and all the matrices are evaluated at $(\xi_{i+1/2}, \eta_{j+1/2}, \zeta_{k+1/2}, \tau_m)$ for the interim step and at $(\xi_{i+1/2}, \eta_j, \zeta_k, \tau_{m+1/2})$ for the regular step.

The mixed implicit-explicit scheme has the following structure:

interim step:

$$\left(\frac{W}{2} + \frac{\Delta\tau_m}{2\Delta\xi} P \right) U_{i+1,j+1/2,k+1/2}^{m+1/2} + \left(\frac{W}{2} - \frac{\Delta\tau_m}{2\Delta\xi} P \right) U_{i,j+1/2,k+1/2}^{m+1/2} = \frac{W}{8} \left(U_{i+1,j+1,k+1}^m \right.$$
$$+ U_{i+1,j,k+1}^m + U_{i+1,j+1,k}^m + U_{i+1,j,k}^m + U_{i,j+1,k+1}^m + U_{i,j,k+1}^m + U_{i,j+1,k}^m + \left. U_{i,j,k}^m \right)$$
$$- \frac{\Delta\tau_m}{2} \left(Q \Delta_\eta U_{i+1/2,j+1/2,k+1/2}^m + R \Delta_\zeta U_{i+1/2,j+1/2,k+1/2}^m \right);$$

regular step:

$$\left(\frac{W}{2} + \frac{\Delta\tau_m}{2\Delta\xi} P \right) U_{i+1,j,k}^{m+1} + \left(\frac{W}{2} - \frac{\Delta\tau_m}{2\Delta\xi} P \right) U_{i,j,k}^{m+1} = \frac{W}{2} \left(U_{i+1,j,k}^m + U_{i,j,k}^m \right)$$
$$- \frac{\Delta\tau_m}{2\Delta\xi} P \left(U_{i+1,j,k}^m - U_{i,j,k}^m \right) - \Delta\tau_m \left(Q \Delta_\eta U_{i+1/2,j,k}^{m+1/2} + R \Delta_\zeta U_{i+1/2,j,k}^{m+1/2} \right),$$

where all the matrices are evaluated at the point $(\xi_{i+1/2}, \eta_{j+1/2}, \zeta_{k+1/2}, \tau_m)$ for the interim step and at the point $(\xi_{i+1/2}, \eta_j, \zeta_k, \tau_{m+1/2})$ for the regular step.

The selection of θ_1, θ_2 and θ_3 in the above schemes is for numerical convenience for the channel flows discussed in this paper. In general, the angles should be chosen such that on the boundary $(\cos\theta_1, \cos\theta_2, \cos\theta_3)$ is the outward normal of the boundary in order to pick up correct equations for the schemes at boundary points, and inside the domain $(\cos\theta_1, \cos\theta_2, \cos\theta_3)$ is the main flow direction.

These schemes have second order truncation errors, thus, accurate numerical results can be expected. The implicit schemes are necessary for the domain between the discontinuities since the CFL number is very close to zero when the discontinuities are very close to each other which causes difficulties for explicit schemes. The scheme is implicit only along the x direction, so we only need to solve a small system of equations along each line.

For interior points, all five equations in (9) are used in the computation. On the left and right boundaries, when p, u, v, w and ρ are given, no equations are needed. Otherwise, the equations corresponding to the characteristic surfaces coming to the boundary from the inside of the domain are needed. On the wall boundaries, the velocities normal to the boundaries are zero and only four equations can be used in the computation, which are the ones corresponding to the characteristic surfaces coming to the boundary from the inside of the domain.

Under the (ξ, η, ζ, τ) coordinate system, the surfaces of discontinuities are the planes $\xi = 1, 2, \cdots, N-1$. When a surface of discontinuity is a shock, all five equations are used to compute the flow parameters p, u, v, w and ρ on the front side of the shock. Behind the shock, there is only one compatibility relation which can be used in the computation. However, the jump conditions (2)-(5) give five more equations. These six equations can be used to determine the flow parameters on the back side of the shock and the new shock speed s. In the case that the discontinuity is a contact discontinuity, there are four compatibility relations on each side of the contact discontinuity respectively, which can be used in the computation. The jump conditions (6) give another three equations. These eleven equations can be used to determine uniquely p, u, v, w, ρ on both sides of the contact discontinuity, and the speed of the contact discontinuity. On a central wave, all five equations are used to find p, u, v, w and ρ. The speed of the central wave surface can be obtained from the speed of the characteristic surfaces.

At each time step, the new positions of the surfaces of discontinuities are determined by the following scheme,

interim step:

$$g^{m+1/2}_{n,j+1/2,k+1/2} = \frac{1}{4}\left(g^m_{n,j,k} + g^m_{n,j+1,k} + g^m_{n,j,k+1} + g^m_{n,j+1,k+1}\right) + \frac{\Delta\tau_m}{8}\left(g^m_{n,\tau,j,k} + g^m_{n,\tau,j+1,k} + g^m_{n,\tau,j,k+1} + g^m_{n,\tau,j+1,k+1}\right);$$

regular step:

$$g^{m+1}_{n,j,k} = g^m_{n,j,k} + \frac{\Delta\tau_m}{4}\left(g^{m+1/2}_{n,\tau,j-1/2,k-1/2} + g^{m+1/2}_{n,\tau,j+1/2,k-1/2} + g^{m+1/2}_{n,\tau,j-1/2,k+1/2} + g^{m+1/2}_{n,\tau,j+1/2,k+1/2}\right),$$

where $g_{n,\tau}$ denote the derivative of $g_n(\eta, \zeta, \tau)$ with respect to τ.

The overall algorithm is as follows:

Before Interaction:

1. In the case of two different family shocks, find $U^m_{i,j,k}$ in the domain between the two shocks. In the case that one discontinuity is a contact discontinuity, find $U^m_{i,j,k}$ in the domains to the two sides of the contact discontinuity.

2. Find $U^m_{i,j,k}$ on the other sides of the discontinuities and the new speeds and positions of the discontinuities by using the relations between the flow fields on the two sides of the discontinuities and a proper characteristic-compatibility relation.

3. Find $U^m_{i,j,k}$ at all other points in the other domain or domains.

4. Adjust $h_i(\eta,\zeta)$ and $k_i(\eta,\zeta)$ after some time steps.

5. Check for breaking down, if the surface τ = constant intersects with any characteristic cone, then stop, the algorithm fails.

At Interaction:

When two discontinuities interact, we need to solve a series of Riemann problems. The algorithm depends on the flow fields on the left of the first discontinuity and on the right of the second discontinuity. In our code, we assume that the flow fields after the interactions could be one of the following cases:

- Case A: Left Shock — Contact discontinuity — Right Shock. Find the flow fields on the right side of the left shock and on the left side of the right shock, i.e., on the two sides of the contact discontinuity. Find the speeds of the left and right shocks, and the contact discontinuity.

- Case B: Left Shock — Contact discontinuity — Right Central Wave or Left Central Wave — Contact discontinuity — Right Shock. Find the flow fields in and behind the central wave, and on the right side of the left shock (left side of the contact discontinuity) or on the left side of the right shock (right side of the contact discontinuity). Find the speeds of the left or right shock, the contact discontinuity, and the central wave.

- Case C: Left Central Wave — Contact discontinuity — Right Central Wave. Find the flow fields in the central wave region and on the two sides of the contact discontinuities, and the speeds of the central wave and the contact discontinuity.

After Interaction:

1. Find $U^m_{i,j,k}$ in the domains to the left of the left discontinuity and to the right of the right discontinuity.

2. Find $U^m_{i,j,k}$ in the central wave region if there is any central wave.

3. Find $U^m_{i,j,k}$ at all points in the domains between the left and right discontinuities (a central wave is also considered as a discontinuity) by using (9) and the relations between the flow fields on the two sides of the discontinuities. Find the new speeds of all discontinuities.

4. Take $h_i(\eta,\zeta)$ = constant in order to change τ back to t.

4. Numerical Results

Several examples has been computed to test the scheme given in the previous section and to compare our method with other methods. Since the limitation of space we give two examples here. In the first example, we computed a two dimensional flow for the purpose of comparison. The flow in the first example has the structure Left Shock — Contact discontinuity — Right Shock after the interactions of the discontinuities. In the second example, we computed a three dimensional flow.

Example 1. consider the channel with a width 0.4, i.e., $y_b = 0.2$. The two discontinuities have the initial positions $x = d_1$ and $x = d_2$, and initial speeds $s_1 = \sqrt{\gamma}\kappa_1(y)$ and $s_2 = \sqrt{\gamma}\kappa_2(y)$, where

$$\kappa_j(y) = s_c^j + \frac{10(s_b^j - s_c^j)|y|^3}{0.2^3} - \frac{15(s_b^j - s_c^j)y^4}{0.2^4} + \frac{6(s_b^j - s_c^j)|y|^5}{0.2^5}, \ -0.2 \le y \le 0.2, \ j = 1, 2,$$

s_c^j and s_b^j, $j = 1, 2$, being parameters. The initial conditions are

$$\begin{aligned}
p_1(x,y) &= \frac{(\gamma(2\kappa_1^2(y) - 1) + 1)(0.5\alpha_1(x) + 0.5)}{\gamma + 1}, \\
u_1(x,y) &= \frac{2\sqrt{\gamma}(\kappa_1^2(y) - 1)(0.1\alpha_1(x) + 0.9)}{(\gamma + 1)\kappa_1(y)}, \qquad v_1(x,y) = 0, \\
\rho_1(x,y) &= \frac{\kappa_1^2(y)(\gamma + 1)(0.5\alpha_1(x) + 0.5)}{2 + (\gamma - 1)\kappa_1^2(y)}, \\
p_2(x,y) &= 1.0, \quad u_2(x,y) = 0.0, \quad v_2(x,y) = 0.0, \quad \rho_2(x,y) = 1.0, \\
p_3(x,y) &= \frac{(\gamma(2\kappa_2^2(y) - 1) + 1)(0.5\alpha_2(x) + 0.5)}{\gamma + 1}, \\
u_3(x,y) &= -\frac{2\sqrt{\gamma}(\kappa_2^2(y) - 1)(0.1\alpha_2(x) + 0.9)}{(\gamma + 1)\kappa_2(y)}, \qquad v_3(x,y) = 0, \\
\rho_3(x,y) &= \frac{\kappa_2^2(y)(\gamma + 1)(0.5\alpha_2(x) + 0.5)}{2 + (\gamma - 1)\kappa_2^2(y)},
\end{aligned}$$

where

$$\alpha_1(x) = 10\sigma^3 - 15\sigma^4 + 6\sigma^5, \qquad \alpha_2(x) = 10\omega^3 - 15\omega^4 + 6\omega^5 \tag{12}$$

with $\sigma = x/d_1$ and $\omega = (1-x)/(1-d_2)$. On the left and right ends of the channel, the boundary conditions are taken as functions of y, which are obtained by setting $x = 0$ and $x = 1$ in the initial conditions. In this example, two shocks exist at the beginning, the left shock is moving to the right, and the right shock is moving to the left. After the interactions, the solution has a structure: Left Shock — Contact discontinuity — Right Shock. The parameters are as follows: $s_c^1 = 2.6$, $s_b^1 = 2.3$, $s_c^2 = 5.0$, $s_b^2 = 5.3$, $d_1 = 0.3$, $d_2 = 0.7$.

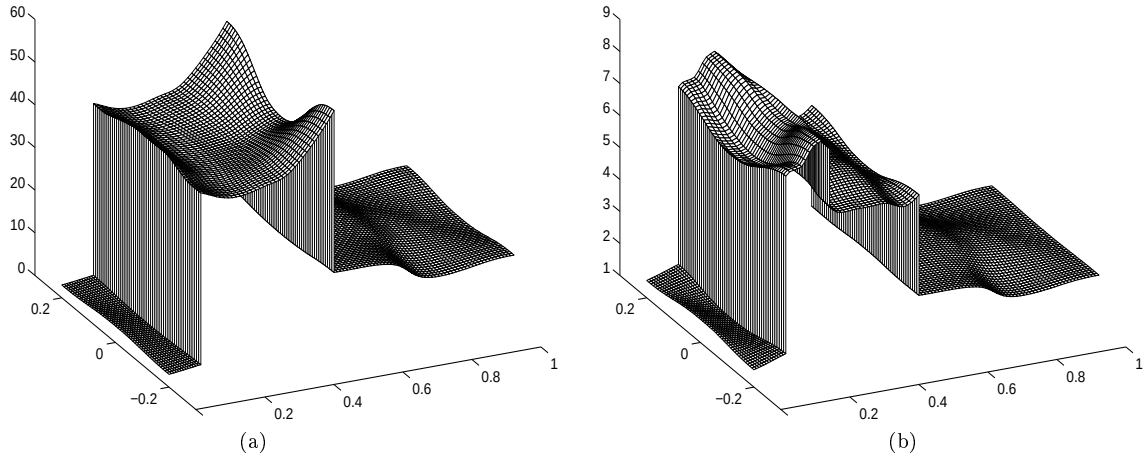

Figure 1: Flow fields at $t = 0.13$ (after interaction),
Fitting, 100×50 mesh, (a) Pressure (b) Density

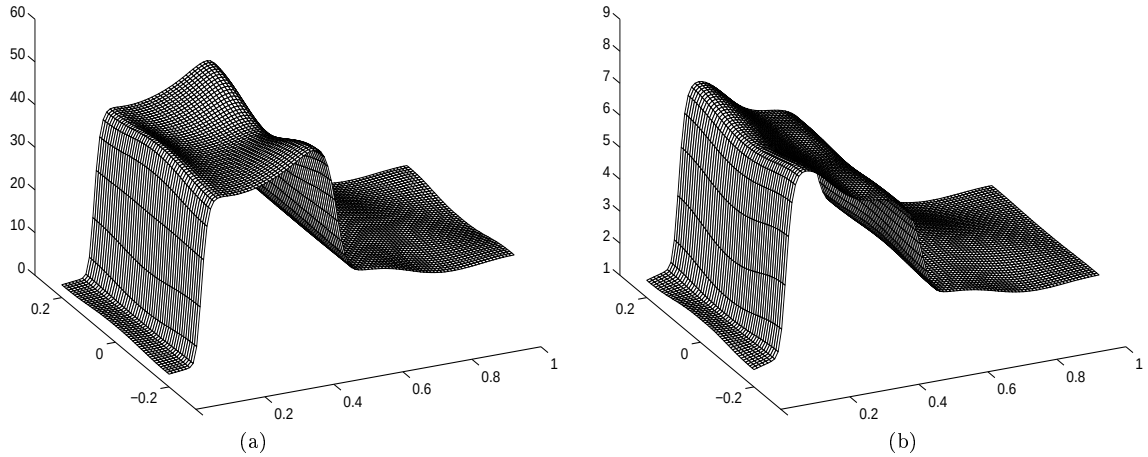

Figure 2: Flow fields at $t = 0.13$ (after interaction),
Lax-Friedrichs, 100×50 mesh, (a) Pressure (b) Density

Figures 1 shows the pressure and density distribution at $t = 0.13$ (after the interactions). The mesh has about 100 points in the x-direction and 50 points in the y-direction, The Fitting scheme represents the method in Section 3. Later on in this paper, similar notations will be adopted. In the figures, all the discontinuities are computed without any smearing or oscillations. In order to compare our method with other methods, we have also computed the same problem by using the Lax-Friedrichs first order scheme and the Essentially Non-oscillatory Lax-Friedrichs third order scheme (ENO-LF3). Figures 2 and 3 show the pressure and density distribution computed by these two schemes. Clearly, the Lax-Friedrichs scheme can not give satisfactory results, the discontinuities are severely smeared. Although the overall results are quite good for the ENO-LF3 scheme, the discontinuities are still smeared. In figures 4 and 5, we show close comparisons among these schemes. Figures 4 shows the comparisons between the pressure and density along the central line at $t = 0.06$. Since across the discontinuities the jumps are big, it is hard for both the Lax-Friedrichs scheme and the ENO-LF3 scheme to catch the discontinuities accurately, but our method gives very accurate results. Figures 5 shows

the similar comparisons at $t = 0.13$. At this time, we can see especially that the ENO-LF3 scheme cannot give sharp transition across the contact discontinuity, the contact discontinuity is severely smeared, while there are no problems with our method.

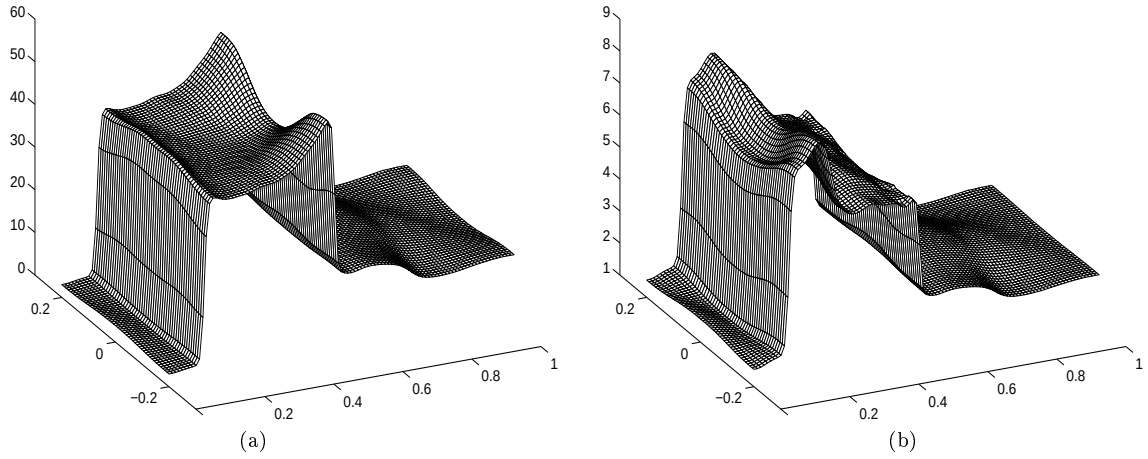

Figure 3: Flow fields at $t = 0.13$ (after interaction), ENO-LF3, 100×50 mesh, (a) Pressure (b) Density

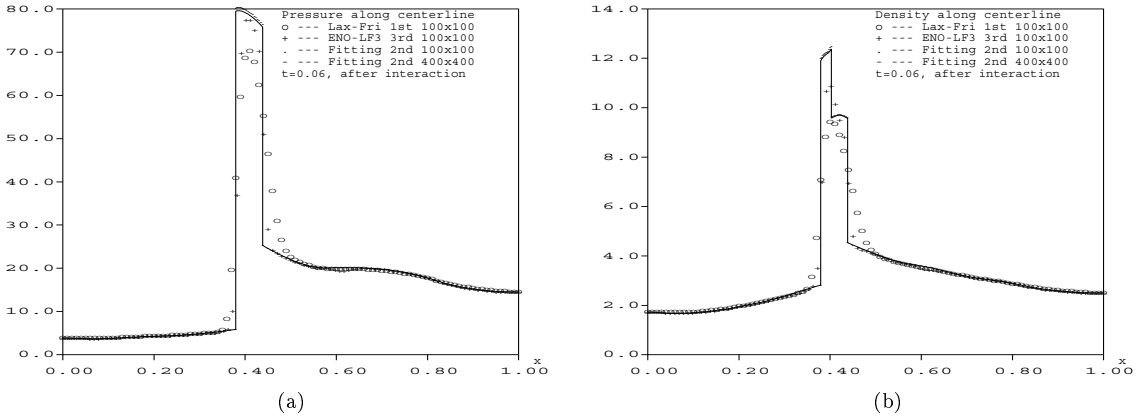

Figure 4: Comparison of Lax-Friedrichs, ENO-LF3 and Fitting schemes, along the centerline, t=0.06, 100×100 mesh, (a) Pressure (b) Density

We also tested the convergence of our method numerically. We first computed the problem on a fine mesh (400 nodes in both spatial directions), and then use this result as the exact solution for comparison. Table 1 shows the relative errors for different meshes under L^1 and L^2 norms. The relative error is defined by $\|U_h - U_e\|_h / \|U_e\|_h$, where U_h is the numerical solution for the corresponding mesh and U_e is the result of the 400×400 mesh. From the tables we can see that the rate of convergence is close to second order both in the L^1 and L^2 norms. The L^1 and L^2 norms of $\|U_h - U_e\|_h$ are computed as follows:

$$\|U_h^m - U_e^m\|_{k,h}^2 = \sum_{i,j} \left|U_{i,j}^m - U(\xi_i, \eta_j, \tau_m)\right|^k \Delta A_{i,j} + \sum_j \left|g_{n,j}^m - g_n(\eta_j, \tau_m)\right|^k \Delta B_j, \qquad k = 1, 2,$$

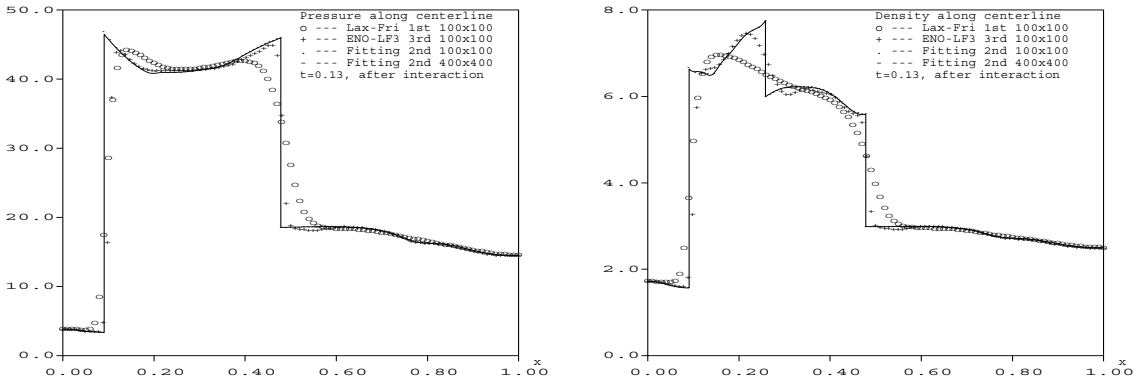

(a) (b)

Figure 5: Comparison of Lax-Friedrichs, ENO-LF3 and Fitting schemes, along the centerline, t=0.13, 100×100 mesh, (a) Pressure (b) Density

Table 1. Relative errors, $t = 0.13$

Meshes	L^1 norm	L^2 norm
50×50	$0.766E-02$	$0.942E-02$
100×100	$0.231E-02$	$0.295E-02$
200×200	$0.758E-03$	$0.995E-03$

where

$$\Delta A_{i,j} = \begin{cases} \Delta\xi\Delta\eta, & \text{for interior points,} \\ \Delta\xi\Delta\eta/2, & \text{for boundary points,} \\ \Delta\xi\Delta\eta/4, & \text{for corner points,} \end{cases}$$

$$\Delta B_j = \begin{cases} \Delta\eta, & \text{for interior points,} \\ \Delta\eta/2, & \text{for boundary points} \end{cases}$$

and the summations about i, j are taken over two domains. The definitions of $\|U_e\|_{1,h}$ and $\|U_e\|_{2,h}$ are similar.

Example 2. The domain is a rectangular channel $[0,1] \times [-0.2, 0.2] \times [-0.2, 0.2]$. At the beginning, the discontinuities have initial positions $x = d_1$ and $x = d_2$, and initial speeds $s_1 = \sqrt{\gamma}\kappa_1(y,z)$ and $s_2 = \sqrt{\gamma}\kappa_2(y,z)$. Here the function $\kappa_1(y,z)$ and $\kappa_2(y,z)$ are symmetric about both y and z axes and defined as follows:

$$\kappa_j(y,z) = \begin{cases} \tilde{\kappa}_j(r), & 0 \le r \le 0.2, \\ s_b^j, & r > 0.2, \end{cases} \qquad j = 1, 2,$$

where

$$\tilde{\kappa}_j(r) = s_c^j + \frac{10(s_b^j - s_c^j)r^3}{0.2^3} - \frac{15(s_b^j - s_c^j)r^4}{0.2^4} + \frac{6(s_b^j - s_c^j)r^5}{0.2^5}, \quad -0.2 \le r \le 0.2, \quad j = 1, 2,$$

s_c^1, s_b^1, s_c^2 and s_b^2 being parameters and $r = \sqrt{y^2 + z^2}$. The initial conditions are

$$
\begin{aligned}
p_1(x,y,z) &= (\gamma(2\kappa_1^2(y,z)-1)+1)(0.5\alpha_1(x)+0.5)/(\gamma+1),\\
u_1(x,y,z) &= \frac{2\sqrt{\gamma}(\kappa_1^2(y,z)-1)(0.1\alpha_1(x)+0.9)}{(\gamma+1)\kappa_1(y,z)},\ v_1(x,y,z)=w_1(x,y,z)=0,\\
\rho_1(x,y,z) &= \frac{\kappa_1^2(y,z)(\gamma+1)(0.5\alpha_1(x)+0.5)}{2+(\gamma-1)\kappa_1^2(y,z)},\\
p_2(x,y,z) &= \rho_2(x,y,z)=1,\ u_2(x,y,z)=v_2(x,y,z)=w_2(x,y,z)=0,\\
p_3(x,y,z) &= (\gamma(2\kappa_2^2(y,z)-1)+1)(0.5\alpha_2(x)+0.5)/(\gamma+1),\\
u_3(x,y,z) &= -\frac{2\sqrt{\gamma}(\kappa_2^2(y,z)-1)(0.1\alpha_2(x)+0.9)}{(\gamma+1)\kappa_2(y,z)},\ v_3(x,y,z)=w_3(x,y,z)=0,\\
\rho_3(x,y,z) &= \frac{\kappa_2^2(y,z)(\gamma+1)(0.5\alpha_2(x)+0.5)}{2+(\gamma-1)\kappa_2^2(y,z)},
\end{aligned}
$$

where $\alpha_1(x)$ and $\alpha_2(x)$ are the same as (12). On the left and right ends of the channel, the boundary conditions are taken as functions of y and z, which are obtained by setting $x=0$ and $x=1$ respectively in the initial conditions. After the interactions, the solution has a structure: Left Shock — Contact Discontinuity — Right Shock. The parameters are taken as: $s_c^1=2.6$, $s_b^1=2.3$ $s_c^2=5.0$, $s_b^2=5.3$, $d_1=0.3$ and $d_2=0.7$.

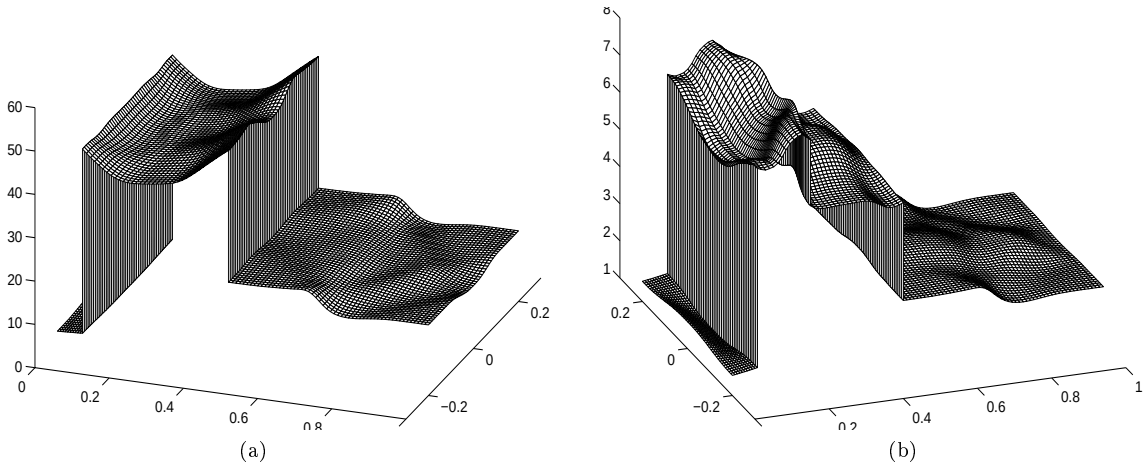

Figure 6: Flow fields on the center surface, $t=0.13$ (after interaction), Fitting, $100\times50\times50$ mesh, (a) Pressure (b) Density

Figure 6 shows the pressure and density distributions on the center surface ($z=0$) for $t=0.13$. Compared with the results in example 1, we can see that our method for three dimensional case is as good as for two dimensional case. In Figure 7 the interaction procedure of the discontinuities is given. (a) shows the two shock surfaces before the interaction. Then at the time $t=0.0445$, (b) shows that the center part of the shock surfaces interacted. The small surface in between the two shock surfaces are the resulting contact discontinuity surface. As the time increases, the part of the interacted discontinuities becomes larger and larger, as shown in (c). Finally, about at $t=0.045$, the interaction is completed. In (d), the three surfaces are the left moving shock, contact discontinuity, and the right moving shock. In (b)

and (c), the interaction is in progress. Thus, the discontinuities are grouped together. To view the discontinuities clearly, we have separated the discontinuity surfaces there.

Finally we point out that examples with central waves have also been tried and the results are as good as these given here.

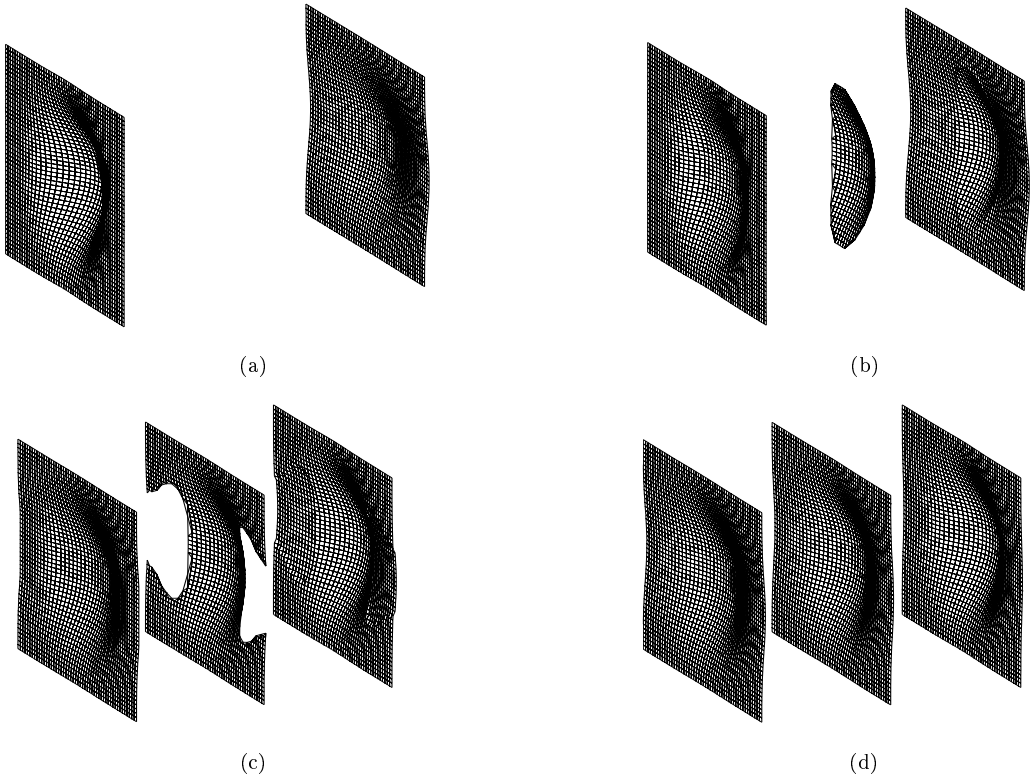

Figure 7: Interactions of discontinuities, (a) $t = 0.043$, shock-shock (b) $t = 0.0445$, shock-contact-shock (c) $t = 0.0447$, shock-contact-shock (d) $t = 0.045$ shock-contact-shock

5. Conclusion

Some two dimensional flow problems with interactions of discontinuities have been computed by the Singularity-Separating method (SSM), the Lax-Friedrichs scheme and the ENO-LF3 scheme. The comparisons show that very accurate numerical results can be obtained if the SSM is used. The paper also shows that some complicated three dimensional results can also be obtained using this method. However, the algorithm presented in this paper has some limitations. As we have seen from the numerical examples, all the test problems considered here have a strong 1D characterization and far to represent complex flows. This is the main weakness of the present algorithm compared to other methods like the front tracking algorithm cited in references [1]-[6]. Therefore, to modify the present algorithm so that it can handle more complicated flow problems like Richtmyer-Meshkov instability [6] would be highly desirable. One possible approach is to combine the present method with some other methods, such as the shock capturing methods.

Acknowledgment. The authors wish to thank Dr. C.-W. Shu for helping in the use of the ENO schemes, and the referees for some valuable comments.

References

[1] J. Glimm, B. Lindquist, Q. Zhang, Front tracking, oil reservoirs, engineering problems and mass conservation, Proceedings of IMA Minisyposium on Computational Issues for Nonlinear Hyperbolic Waves, April 17-21, 1989.

[2] J. Glimm, A review of interface methods for fluid computations, SUNY at Stony Brook, Dept. of Applied Mathematics and Statistics, No. SUNYSB-AMS-90-07, 1990.

[3] I.-L. Chern, J. Glimm, O. McBryan, B. Plohr, D.H. Sharp, Front tracking for gas dynamics, *J. Comput. Phys.,* **62** (1986), 83-110.

[4] J. Glimm, X.L. Li, R. Menikoff, D.H. Sharp, Q. Zhang, A numerical study of bubble interactions in Rayleigh-Taylor instability for compressible fluids, Physical Fluids A, 2 (1990).

[5] John W. Grove, R. Menikoff, Anomalous reflect of a shock wave at a fluid interface, *J. Fluid Mech.,* **219** (1990), 313-336.

[6] Richard L. Holmes, John W. Grove, David H. Sharp, Numerical investigation of Richtmyer-Meshkov instability using front tracking, *J. Fluid Mech.,* **301** (1995), 51-64.

[7] G. Moretti, Three-dimensional supersonic, steady flows with any number of embedded shocks, AIAA paper 74-10, Washington D.C., 1974.

[8] De-kang Mao, A treatment of discontinuities for finite difference methods in the two-dimensional case, *J. Comput. Phys.,* **104** (1993), 377-397.

[9] You-lan Zhu, Xi-chang Zhong, Bing-mu Chen, Zuo-min Zhang, Difference Methods for Initial-Boundary Value Problems and Flow Around Bodies, Springer-Verlag, Heidelberg and Sciences Press, Beijing, 1988.

[10] You-lan Zhu, Bing-mu Chen, A numerical method with high accuracy for calculating the interactions between discontinuities in three independent variables, *Scientia Sinica,* **23** (1980).

[11] P.D. Lax, Weak solution of non-linear hyperbolic equations and their numerical computation, *Comm. Pure Appl. Math.,* **7** (1954), 159-193.

[12] Chi-Wang Shu, Stanley Osher, *Efficient implementation of essentially non-oscillatory shock capturing schemes II, J. Comput. Phys.,* **83** (1989), 32-78.

[13] Xiaonan Wu, Youlan Zhu, A highly accurate numerical method for two and three dimensional shock reflection problems, *Computers & Fluids,* **25** (1996), 295-317.